MAP4 Is the in Vivo Substrate for CDC2 Kinase in HeLa Cells: Identification of an M-Phase Specific and a Cell Cycle-Independent Phosphorylation Site in MAP4[†]

Kayoko Ookata,[‡] Shin-ichi Hisanaga,*[,‡] Minoru Sugita,[‡] Akira Okuyama,[§] Hiromu Murofushi,[||] Hidefumi Kitazawa,[‡] Sripriya Chari,[⊥] Jeannette Chloe Bulinski,[⊥] and Takeo Kishimoto[‡]

Laboratory of Cell and Developmental Biology, Faculty of Biosciences, Tokyo Institute of Technology, 4259 Nagatsuta, Midori-ku, Yokohama 226, Japan, Banyu Tsukuba Research Institute Collaboration with Merck Research Institute, 3 Okubo, Tsukuba 330-33, Japan, Department of Biophysics and Biochemistry, Faculty of Science, The University of Tokyo, Hongo, Tokyo 113, Japan, and Department of Anatomy and Cell Biology, College of Physicians and Surgeons of Columbia University, New York, New York 10032

Received May 28, 1997; Revised Manuscript Received September 10, 1997[⊗]

ABSTRACT: We reported previously that cdc2 kinase decreased the microtubule-stabilizing ability of a major HeLa cell microtubule-associated protein, MAP4, by phosphorylation *in vitro* [Ookata, K., et al. (1995) *J. Cell Biol. 128*, 849−862]. An important question raised by this study is whether MAP4 is indeed phosphorylated by cdc2 kinase at mitosis *in vivo*. We present here evidence that cdc2 kinase is the major M-phase MAP4 kinase, and, further, we identify two phosphorylation sites within the proline-rich domain of MAP4. Metabolic ^{32}P labeling showed the increased phosphorylation of MAP4 at mitosis. A specific inhibitor of cdc2 kinase, butyrolactone I, inhibited phosphorylation of MAP4 both in mitotic HeLa cells and in the mitotic HeLa cell extract. The phosphopeptide map analysis revealed the high similarity of *in vivo* labeled mitotic MAP4 to that phosphorylated by cdc2 kinase *in vitro*. Ser-696 and Ser-787, both of which lie within SPXK consensus sequences for cdc2 kinase, were identified as phosphorylation sites in the proline-rich region of MAP4 *in vivo* and *in vitro*. Immunoblotting with antibodies that recognize the phosphorylation state of Ser-696 or Ser-787 showed that Ser-787 in the SPSK sequence was specifically phosphorylated at mitosis while Ser-696 in the SPEK sequence was phosphorylated both at mitosis and in interphase. These results suggest that cdc2 kinase directly regulates microtubule dynamics at mitosis through phosphorylation of MAP4 at a number of sites, including Ser-787.

The architecture of the microtubule cytoskeleton in eukaryotic cells changes dramatically at mitosis. Interphase cytoplasmic microtubules, which emanate radially from the centrosome located adjacent to nucleus to the cell periphery, transiently depolymerize and then are reorganized into mitotic spindles at the onset of mitosis (*1*, *2*). This reorganization may depend on coordinated alterations in both the microtubule nucleating activity of the centrosomes and the dynamic property of microtubules. These mitotic changes have been reported to be regulated by protein phosphorylation at mitosis (*3*−*6*). The protein kinases most often implicated in controlling microtubule dynamics are $p34^{cdc2}$/cyclin B kinase (cdc2 kinase) and MAP kinase. In fact, microtubule dynamics in *Xenopus* egg extracts were stimulated when the extracts were brought to the mitotic state from the interphase by the addition of truncated cyclin B protein or cdc2 kinase (*4*, *7*, *8*) and in sea urchin eggs induced to a mitotic-like state by okadaic acid (*6*). MAP kinase is also activated at mitosis in *Xenopus* oocytes (*9*). Phosphorylation of MAPs by either cdc2 kinase or MAP kinase affects their ability to stimulate microtubule polymerization (*10*−*14*).

Microtubule dynamics is modulated by microtubule-associated proteins (MAPs) (*15*−*17*). Heat-stable MAPs from mammalian brain, MAP2 and tau, have been studied extensively; they are able to induce polymerization of tubulin and stabilize microtubules both *in vivo* and *in vitro* (*18*−*20*). Their phosphorylation is known to reduce their microtubule-polymerizing and -stabilizing abilities (*21*−*23*). Despite these well-known *in vitro* biochemical properties, however, the physiological role of MAP phosphorylation in neurons is not known. Proliferating cells, such as mammalian non-neuronal cells grown in tissue cultures, contain a heat-stable MAP, called MAP4, which is an abundant MAP with properties and structure similar to MAP2 and tau (*24*−*28*). In these proliferating cells, immunoblotting with MPM2 antibody, a monoclonal antibody reactive with mitosis-specific phosphorylated epitopes, suggested that MAP4 is phosphorylated at mitosis, concomitant with the increase in microtubule dynamics (*29*, *30*). Thus, proliferating cells can

[†] This work was supported by grants from the American Cancer Society and the Council for Tobacco Research (J.C.B.), the Ministry of Education, Science, and Culture in Japan (S.H. and T.K.), and CREST, Japan Science and Technology Corporation (JST) (T.K.).

* All correspondence should be addressed to this author at the present address: Department of Biology, Faculty of Science, Tokyo Metropolitan University, Minamiosawa 1-1, Hachiohji-shi, Tokyo 192-03, Japan. Tel: +81-426-77-2577. Fax: +81-426-77-2559. E-mail: hisanaga-shinichi@c.metro-u.ac.jp.

[‡] Tokyo Institute of Technology.

[§] Banyu Tsukuba Research Institute in Collaboration with Merck Research Institute.

[||] The University of Tokyo.

[⊥] College of Physians and Surgeons of Columbia University.

[⊗] Abstract published in *Advance ACS Abstracts,* November 15, 1997.

[1] Abbreviations: BL-I, butyrolactone I; cdc2 kinase, $p34^{cdc2}$/cyclin B kinase; MAP4, microtubule-associated protein 4; MAP kinase, mitogen-activated protein kinase; GSK3, glycogen synthase kinase 3; SDS−PAGE, sodium dodecyl sulfate−polyacrylamide gel electrophoresis.

S0006-2960(97)01251-8 CCC: $14.00

provide a good experimental system to correlate the phosphorylation of MAPs to dynamic behavior of microtubules *in vivo* (*31*). We recently demonstrated that phosphorylation of MAP4 by cdc2 kinase reduced its microtubule-stabilizing activity *in vitro* and that cdc2 kinase associated with microtubules through direct binding of cyclin B to MAP4 (*14*). However, MAP4 has been shown to be phosphorylated by MAP kinase and protein kinase C *in vitro* (*12*, *32*). Thus, an important question is whether MAP4 is indeed phosphorylated by cdc2 kinase at mitosis *in vivo*. In this study, we addressed this question using HeLa cells. Somatic cultured cells present an advantage for determining those kinases active on MAP4 in mitosis, little if any activation of MAP kinase has been demonstrated in HeLa cells, in contrast to the meiotic and early embryonic M-phase, in which full activation of MAP kinase occurs (*9*, *33*). In this paper, we show evidence that cdc2 kinase is a major mitotic MAP4 kinase and that Ser-787 of MAP4 could be one of the phosphorylation sites responsible for regulation of microtubule-stabilizing ability. We further show the occurrence of cell cycle-independent phosphorylation on Ser-696 of the MAP4 molecule.

MATERIALS AND METHODS

Cell Culture and Metabolic Phosphorylation of MAP4

HeLa cells were cultured and synchronized as described previously (*14*). HeLa cells synchronized at mitosis or asynchronous, log phase HeLa cells were labeled in the presence of approximate 9 MBq/mL [^{32}P]orthophosphoric acid in phosphate-free DME culture medium containing 5% dialyzed fetal calf serum, with or without 30−50 μM of butyrolacetone-I (BL-I) for 3 h.

Preparation of in Vivo Labeled MAP4

After washing with PBS(−) (Nissui, Tokyo, Japan), HeLa cells were lysed in 3 vol of extraction buffer [50 mM imidazole, pH 6.8, 50 mM NaF, 50 mM β-glycerophosphate, 1 mM EGTA, 1 mM $MgCl_2$, 0.5% Nonidet P-40, 1 μg/mL leupeptin, 1 μg/mL pepstatin, 0.1 mM phenylmethylsulfonyl fluoride (PMSF), and 1 mM dithiothreitol (DTT)] and frozen with liquid nitrogen. After being thawed quickly, the lysate was centrifuged at 100000*g* for 30 min at 2 °C. The supernatant was boiled for 5 min followed by centrifugation at 100000*g* for 30 min.

The heat stable supernatant was diluted 4-fold with 50 mM Pipes, pH 6.8, 1 mM EGTA, and 1 mM $MgCl_2$ (50PEM) containing 10 μM paclitaxel and 0.5 mM GTP, mixed with microtubules which had been polymerized from purified porcine brain tubulin with 20 μM paclitaxel and 0.5 mM GTP, and were incubated at 30 °C for 10 min. Microtubules were collected by centrifugation at 40000*g* for 30 min at 30 °C. The pelleted microtubules were suspended with 0.5 M NaCl and boiled for 5 min. After clarification by centrifugation at 100000*g* for 30 min, the heat-stable MAP fraction was processed for autoradiography or 2D phosphopeptide map analysis after SDS−PAGE.

In vivo phosphorylated MAP4 was also isolated by immunoprecipitation with an anti-bovine MAP4 antibody (*34*). A 30 μL amount of the heat-stable supernatant was added to 75 μL of affinity-purified anti-MAP4 antibody that had been diluted 15-fold with the immunoprecipitation buffer (50 mM Tris-HCl, pH 7.5, 150 mM NaCl, 1 μg/mL leupeptin, 1 μg/mL pepstatin, 0.1 mM PMSF, and 1 mM DTT) and incubated for 60 min at 4 °C. A 50% slurry of protein A-Sepharose CL-4B (Pharmacia, Uppsala, Sweden), 20 μL, was added, and the mixture was incubated further for 60 min at 4 °C. Sepharose beads were pelleted by centrifugation at 12000*g* for 3 min at 4 °C and washed three times with immunoprecipitation buffer and then three times with immunoprecipitation buffer containing 0.05% Tween 20 and 0.5 M NaCl. Washed Sepharose beads were added to 10 μL of H_2O and 10 μL of 4× SDS sample buffer. After being boiled for 2 min and then centrifuging at 12000*g* for 10 min, the supernatant was processed for SDS−PAGE and autoradiography.

The HeLa cell heat-stable supernatant used for immunoblotting with anti-MAP4 antibodies was prepared by boiling a HeLa cell homogenate in 10 mM HEPES, pH 7.4, 1 mM EGTA, 0.75 M NaCl, 0.5% Nonidet P-40, and 10% sucrose, followed by centrifugation at 100000*g* for 30 min at 4 °C.

Preparation of MTB1, MTB2, and MTB3

Preparation of a pET expression plasmid (*35*) whose cDNA insert encodes full-length, five-repeat MAP4 [pET-MAP4-5r; see Chapin et al. (*27*) for terminology and sequences] has been described in Nguyen et al. (*36*). To prepare pET-MTB2, pET-MAP4-5r was cut with *Stu*I and blunt-end religated in the prsence of an eight base pair *Xho*I linker. This construct was checked by measuring the size of pET-MTB2 cut with *Xho*I to detect the new site, and BsteII site. To prepare MTB1, a 5′ primer containing an *Xho*I site was designed (CCAGCCTCCTCGAGTGGGTCCAAG) and used in PCR, with a template of pET-MAP4-5r, along with a 3′ primer (TCATCATTAGATGCTTGTCTCCTGGAT) situated 3′ to MAP4's unique *Bste*II site. PCR fragments were cut with *Xho*I site and *Bste*II and ligated into pET-MTB2 that had been cut with the same two enzymes. Again, *Xho*I and *Bste*II were used to check the size of the insert. To prepare pET-MTB3, the same strategy was used except that, in the PCR reaction with full-length MAP4 as template, the following 5′ primer was used: CTTCAGAGACCTCGAGAATAG. pET-MTB1, -2, and -3 were transformed into BL-21 bacteria and grown and induced as previously described (*36*).

MTB1 (amino acid residues 800−1152) or MTB2 (amino acid residues 763−1152) was purified from the extract of *Escherichia coli* carrying pET-MTB1 or pET-MTB2 plasmid, respectively, by a Mono-S column (Pharmacia). MTB3 (amino acid residues 668−1152) was purified from a heat-stable fraction of the extract prepared from bacterial cells carrying pET-MTB3 plasmid, using a Mono-S column.

Preparation of Other Proteins

Microtubule protein was prepared from porcine brains by two cycles of temperature-dependent polymerization/depolymerization (*37*). Tubulin was purified from microtubule preparations by phosphocellulose column chromatography (*38*).

HeLa crude MAP4 were prepared from asynchronously growing cells or mitotic cells by the same method as described previously (*14*, *39*).

Cdc2 kinase was purified from starfish oocytes at the first meiotic M-phase or Nocodazole-arrested mitotic HeLa cells

by p13^{suc1} affinity column chromatography (*40*, *41*). Glycogen synthase kinase 3β (GSK3β) was purchased from New England Biolabs Inc. (Beverly, MA). *E. coli* carrying *Xenopus* MAP kinase cDNA was provided by Dr. Eisuke Nishida (Kyoto University, Kyoto, Japan). Bacterially expressed MAP kinase was purified and activated by thiophosphorylation with *Xenopus* MAP kinase kinase as described previously (*42*).

Kinase Assay

HeLa cell extracts for the kinase assay were prepared by freeze−thawing in 20 mM MOPS, pH 6.8, 0.5 M NaCl, 5 mM EGTA, 1 mM $MgCl_2$, 0.1 mM DTT, 20 mM β-glycerophosphate, 10% sucrose, and 0.5% Nonidet P-40, followed by centrifugation at 100000*g* for 30 min at 4 °C.

Histone H1 (0.2 mg/mL) and crude MAP4 (120 μg/mL) were phosphorylated using 0.1 mM [γ-^{32}P]ATP and mitotic HeLa cell extracts in the presence or absence of 25 μM BL-I at 30 °C for 10 min. The reaction was stopped by the addition of the SDS−PAGE sample buffer or by boiling. Phosphorylation was monitored by autoradiography following SDS−PAGE.

HeLa MAP4 (50 μg/mL) was phosphorylated by cdc2 kinase, GSK3β, or MAP kinase in 50PEM containing 0.1 mM [γ-^{32}P]ATP at 30 °C for 60 min. The reaction was stopped by addition of SDS−PAGE sample buffer, and phosphorylated MAP4 was subjected to 2D phosphopeptide map analysis, following SDS−PAGE.

Oligopeptides were synthesized to mimic parts of the amino acid sequence of MAP4: 691−700 (KELPPSPEKK) and 782−791 (PEKRASPSKP) (*26*, *27*), with two Arg residues added to the N-terminal end of each. Synthetic peptides (0.1 mg/mL) were phosphorylated by cdc2 kinase (5 μg/mL) or the catalytic subunit of cAMP-dependent protein kinase, in reaction medium consisting of 0.1 mM [γ-^{32}P]ATP, 1 mM $MgCl_2$ and 20 mM MOPS, pH 7.2, at 37 °C. The reaction was stopped by spotting 5 μL of reaction mixture on phosphocellulose paper, and the incorporated ^{32}P was measured by liquid scintillation counting.

Dephosphorylation of MAP4

HeLa cell mitotic MAP4, which was dialyzed against 20 mM Tris-HCl, pH 8.5, 0.1 mM EGTA, and 0.15 M NaCl, was dephosphorylated by incubation with 50 units/mL of *E. coli* alkaline phosphatase (Wako, Osaka, Japan) at 67 °C for 1 or 2 h.

Two-Dimensional Phosphopeptide Map Analysis

Two-dimensional phosphopeptide map analysis was carried out as described by Boyle et al. (*43*). *In vivo* labeled MAP4 and MAP4 phosphorylated by cdc2 kinase *in vitro* were separated on SDS−PAGE. After the gels were stained with Coomassie Brilliant Blue, MAP4 was excised and digested with 0.1 unit/mL lysylendopeptidase in 50 mM NH_4HCO_3 for 16−24 h at 37 °C. Peptides phosphorylated by cdc2 kinase were bound to phosphocellulose paper, and after being washed with 1% phosphoric acid, peptides were released from the papers, by digestion with lysylendopeptidase in 50 mM NH_4HCO_3, pH 8.5. After the digested peptides were concentrated by lyophilization, phosphopeptides were electrophoresed in the first dimension at pH 3.5 and then subjected to ascending chromatography in isobutyric acid:pyridine:acetic acid:*n*-butanol:H_2O (1251:96:58:38:557); 500−1500 cpm, measured by Cerenkov counting, was applied to a silica gel thin-layer plate (Merck, Darmstadt, Germany). After the TLC plate was dried, phosphopeptides were detected with a BAS 2000 image analyzer (Fuji Film, Tokyo, Japan).

Antibodies and their Affinity Purification

Anti-phospho-S^{696}PEK and anti-phospho-S^{787}PSK antibodies were raised in rabbits against a synthetic phosphopeptide, KELPPS(PO_4)PEKK or PEKRAS(PO_4)PSKP coupled to keyhole limpet hemocyanin. A 50 μg of amount of peptide emulsified with Freund's complete adjuvant was injected as the first immunization, and then those emulsified with Freund's incomplete adjuvant were injected three times at two-week intervals. The rabbits were bled 1 week after the last injection.

Anti-phospho-S^{696}PEK and anti-phospho-S^{787}PSK antibodies were affinity-purified on a column of the appropriate phosphopeptide, coupled to CNBr-activated Sepharose CL-4B, after removal of phosphorylation-independent antibody populations on Sepharose column coupled with the unphosphorylated version of each peptide.

SDS−PAGE and Western Blotting

SDS−PAGE was performed accordingly to Laemmli (*44*). Separated proteins were transferred to Immobilon membranes (Millipore Corp., Bedford, MA). Those blots probed with anti-MAP4, and anti-phospho-S^{696}PEK and anti-phospho-S^{787}PSK antibodies were labeled with alkaline phosphatase-conjugated secondary antibody and developed with a BCIP/NBT phosphatase substrate system (*45*).

Adsorption of antibodies was performed by incubation with 5 μg/mL of unphosphorylated or phosphorylated peptides in 4% skim milk/Tris-buffered saline for 60 min at room temperature.

RESULTS

MAP4 is Phosphorylated by cdc2 Kinase in Mitotic HeLa Cells

Previous reports have suggested that MAP4 is phosphorylated at mitosis, because it is immunoreactive with MPM2, an antibody that recognizes M-phase-specific phosphorylated epitopes and because M-phase MAP4 exhibits an upward shift in its electrophoretic mobility (*29*, *30*). We confirm the M-phase specific phosphorylation of MAP4 in Figure 1A, in which a slight decrease in electrophoretic mobility can be seen for M-phase MAP4. We examined phosphate incorporation into MAP4 in HeLa cells by metabolic ^{32}P-labeling; we prepared MAP4 from labeled extracts by preparing a heat-stable supernatant fraction of the cell lysate and binding the MAP to microtubules or immunoprecipitating it with an anti-MAP4 antibody. Two phosphorylated bands were detected at 200 and 120 kDa in the heat-stable MAP fraction of the HeLa extract (Figure 1B). The band with molecular mass 200 kDa was phosphorylated to a much greater degree (about 7−8 times estimated by a Image Analyzer) in mitotic cells than in asynchronous cells (Figure 1B). This 200 kDa band is probably MAP4, judging from its electrophoretic mobility, which is identical with the anti-MAP4 immunoreactive band (Figure 1A). The 120 kDa

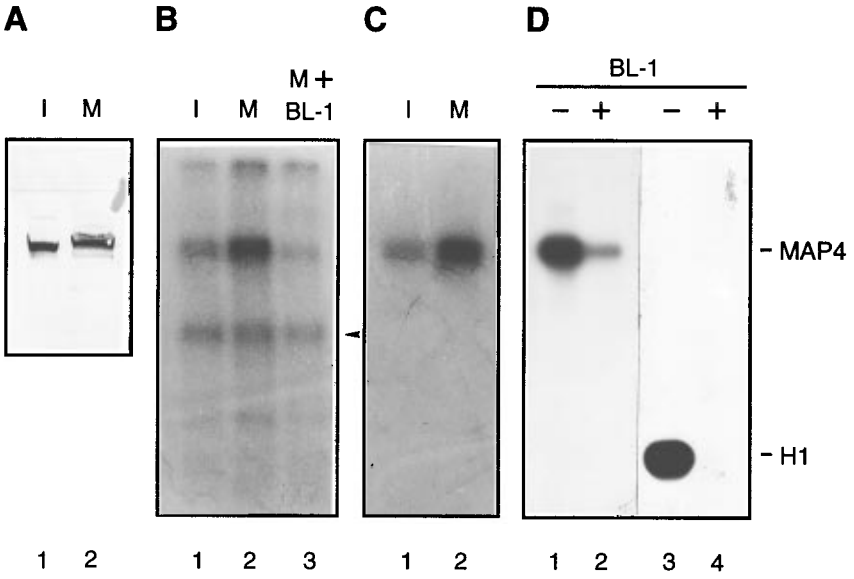

FIGURE 1: Mitosis-specific phosphorylation of MAP4 in HeLa cells. (A) shows an immunoblot of mitotic (M) and interphase (I) HeLa cell extracts with anti-bovine MAP4 antibody. M-phase MAP4 showed a slightly slower mobility than interphase MAP4, as reported previously by Tombes et al. (*30*) and Vandre et al. (*29*). Mitotic and interphase HeLa cells were cultured in the presence of [^{32}P]orthophosphate for 3 h. MAP4 was prepared from heat-stable supernatants of HeLa cells by binding to microtubules (B) or by immunoprecipitation with anti-MAP4 antibody (C), and then autoradiographed after SDS−PAGE. Mitotic MAP4 (B and C, lane 2) was phosphorylated to a much greater extent than interphase MAP4 (B and C, lane 1). Phosphorylation of MAP4 at mitosis was inhibited in the presence of 50 μM BL-I (B, lane 3), which was added at the same time as the addition of [^{32}P]orthophosphate. Arrowhead indicates the 120 kDa phosphorylated protein which may correspond to another HeLa MAP named ensconsin or E-MAP115 (*46*−*48*). (D) Phosphorylation of MAP4 in mitotic HeLa extracts and its inhibition by BL-I. MAP4 prepared from asynchronous HeLa cells was phosphorylated in the mitotic HeLa extract in the absence (lane 1) or presence (lane 2) of 20 μM BL-I. Phosphorylation of MAP4 was inhibited by BL-I with the same concentration required to inhibit phosphorylation of histone H1 (lanes 3 and 4).

band (arrowhead in Figure 1B), which was phosphorylated both in the interphase and M-phase, may correspond to another HeLa MAP named ensconsin (*46*) or E-MAP115 (*47*, *48*). Mitotic phosphorylation of MAP4 was confirmed with immunoprecipitation, using affinity-purified anti-MAP4 antibody (Figure 1C).

One can easily envisage that MAP4 is phosphorylated by a kinase activated at mitosis, and cdc2 kinase is the most probable candidate for such a kinase. To test this possibility, we used specific inhibitor of cdc2 kinase, butyrolactone-I (BL-I) (*49*). In cell culture, BL-I was shown to inhibit the entry of HeLa cells into mitosis, when we used a concentration of greater than 20 μM BL-I (H. Shimosakai, T.K., and S.H., unpublished observation). BL-I (50 μM) was added to the culture medium at the time of activation of cdc2 kinase (9 h after thymidine release) together with [^{32}P]orthophosphate. Phosphorylation of MAP4 was inhibited in the presence of BL-I (Figure 1B, lane 3), indicating that the activity of cdc2 kinase is required for MAP4 phosphorylation.

However, from this result it is still not clear whether cdc2 kinase itself or a kinase downstream of cdc2 kinase phosphorylates MAP4. To resolve this question, we examined phosphorylation of MAP4 in mitotic HeLa extracts, which would be expected to contain most kinases active at M-phase, in the presence or absence of BL-I to inhibit cdc2 kinase. BL-I inhibited phosphorylation of MAP4 in mitotic HeLa cell extracts, at a concentration of 20 μM (Figure 1D, lanes 1 and 2); at this concentration phosphorylation of histone H1 in mitotic cell lysates was also inhibited (Figure 1D, lanes 3 and 4).

These results indicate that the major mitotic MAP4 kinase is cdc2 kinase. We further confirmed this by two dimensional phosphopeptide map analysis. *In vivo* labeled MAP4 was separated by SDS−PAGE, digested with protease, and the resulting phosphopeptides were compared with those of MAP4 phosphorylated by cdc2 kinase *in vitro*. Mitotic MAP4 yielded five major phosphorylated peptides (Figure 2A and D, spots numbered 1, 4, 6, 9, and 10) and three minor phosphorylated peptides (Figure 2A and D, spots numbered 2, 3, and 5). MAP4 phosphorylated by cdc2 kinase *in vitro* produced a phosphopeptide pattern (Figure 2B) strongly resembling that of *in vivo* phosphorylated MAP4 (Figure 2A). To compare the phosphorylated peptides more clearly, we electrophoresed a mixture of them, as shown in Figure 2C. Five of the *in vivo* phosphorylated peptides comigrated with *in vitro* phosphorylated peptides of MAP4 (Figure 2C, spots 4, 5, 6, 9, and 10), indicating that MAP4 was mainly, but not exclusively, phosphorylated by cdc2 kinase in mitotic HeLa cells.

cdc2 kinase is a proline-directed kinase, phosphorylating a Ser or Thr residue followed by a Pro residue. There are at least two other proline-directed kinases: mitogen-activated protein kinase (MAP kinase) and glycogen synthase kinase 3 (GSK3) (*50*, *51*). These three kinases have a overlap substrate specificity. To test the possibility that MAP4 is phosphorylated by MAP kinase or GSK3β, 2D phosphopeptide maps of MAP4 phosphorylated by these kinases were compared. MAP kinase phosphorylated MAP4, as reported by Hoshi et al. (*12*), but its major phosphorylation spots were different from that of mitotic phosphorylation, except for two minor spots that appeared to comigrate with spot 5 and spot 6 (Figure 2E). GSK3β showed a poor kinase activity against MAP4. Compared with tau, a well-known substrate for GSK3β, MAP4 was phosphorylated less than one-tenth as much, when a similar concentration of proteins was used for the kinase assay. The only phosphorylation spot obtained

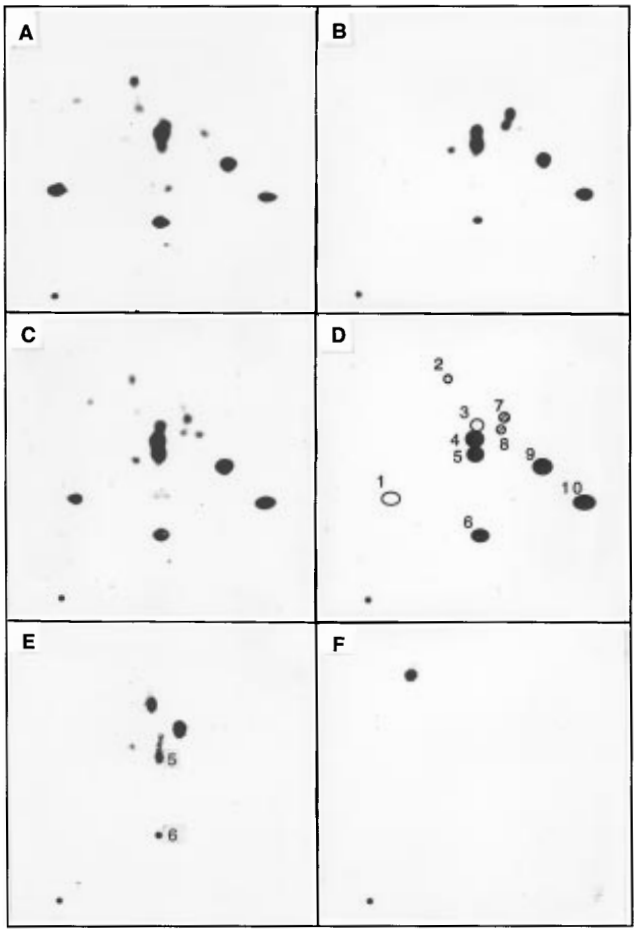

FIGURE 2: 2D phosphopeptide map of mitotic MAP4 resembles that of MAP4 phosphorylated by cdc2 kinase *in vitro*. 2D phosphopeptide mapping of MAP4 labeled in mitotic HeLa cells (A) was compared with that of MAP4 phosphorylated *in vitro* by cdc2 kinase (B), MAP kinase (E), or GSK3β (F). C is a superimposition of A and B, while D shows a schematic representation of C. Numbers indicate individual phosphopeptides: spots 1−3 (open circles) are peptides specifically phosphorylated *in vivo*, spots 7 and 8 (dashed circles) are peptides specifically phosphorylated *in vitro* by cdc2 kinase, and spots 4−6, 9, and 10 (filled circles) are peptides common in both *in vivo* and *in vitro* phosphorylated MAP4. The origin is in the lower left corner of each TLC plate. Five (4−6, 9, and 10) of the eight (1−6, 9, and 10) major *in vivo* phosphopeptides comigrated with those phosphorylated by cdc2 kinase *in vitro*. Phosphorylation by MAP kinase (E) or GSK3β (F) showed a different 2D phosphopeptide pattern from the mitotic phosphorylation. Spots corresponding to 5 and 6 are labeled in E.

migrated at the upper-left portion of 2D-map (Figure 2F), a site which no mitotic spots migrated. Therefore, these two proline-directed kinases are apparently not responsible for the major mitotic phosphorylation of MAP4, although the possibility that these contribute in a minor way cannot be ruled out.

Identification of cdc2 Kinase Phosphorylation Sites in MAP4

The sequence (S/T)-P-X-(K/R) has been proposed to be the consensus sequence for phosphorylation by cdc2 kinase (*52*). There are six such sequences in the human MAP4 molecule (Figure 3A). Four sites are present in the amino-terminal projection domain, and two are located in the proline-rich region in the C-terminal half. No consensus sequences are present within the microtubule binding repeats or the extreme carboxy-terminus of human MAP4 protein. We focused our attention on Ser-696 in the SPEK sequence and Ser-787 in the SPSK sequence [numbered according to West et al. (*26*) and Chapin et al. (*27*)] because both of these are located in the so-called Pro-rich region, which has been shown to be involved in binding of MAP4 to microtubules (*53*, *54*). Further, the amino acid sequences of these two sites are conserved in human, bovine and rat MAP4 protein (*26*, *27*, *55*); phosphorylation sites involved in mitotic progression would be expected to be conserved among different species.

To determine whether Ser-696 and Ser-787 can be phosphorylated by cdc2 kinase and, if so, to identify their positions in 2D phosphopeptide maps, we constructed three human MAP4 fragments containing C-terminal domains of different lengths (Figure 3A); MTB1 (amino acid residues 800−1152, containing no consensus sequence for cdc2 kinase), MTB2 (amino acid residues 763−1152, containing Ser-787) and MTB3 (amino acid residues 668−1152, containing both Ser-696 and Ser-787). Each fragment was phosphorylated by cdc2 kinase (Figure 3B). MTB1 was phosphorylated even though it contains no (S/T-P-X-(R/K) consensus sequence. Since it contains three TP and one SP sequences (Figure 3A, four arrowheads behind Ser-787), however, it is possible that cdc2 kinase phosphorylates some of these motifs.

After digestion with lysylendopeptidase, the resultant peptides were subjected to 2D phosphopeptide mapping. MTB3 generated three major and three moderate spots (Figure 3E) that were reminiscent of the 2D-phosphopeptide map (Figure 2B) of interphase MAP4 phosphorylated by cdc2 kinase. When two characteristic spots at the upper right corner of the map were adjusted to spots 7 and 8 in Figure 2B and D, the two major spots vertically aligned at the center were shown to correspond to spots 4 (large arrow) and 5 of Figure 2B, and another major spot at the lower-right corner (indicated by arrow) was shown to move to the position of spot 10. In comparing the phosphopeptide maps of MTB1, MTB2, and MTB3, the most striking features are that spot 4 disappeared in the 2D map of MTB1 and MTB2 (Figure 3C and D), suggesting that spot 4 contains Ser-696 as a phosphorylation site. In the 2D map of MTB1, spot 10 was missing (Figure 3C), suggesting that spot 10 is the peptide containing Ser-787. Three moderate phosphorylation spots in Figure 3E (two spots at the upper right corner and a spot at the left side of two major spots vertically aligned at the center) were intense in the absence of better phosphorylation sequences not included in MTB fragments (Figure 3C). This result indicates that S-P or T-P sequences can be recognized in *in vitro* phosphorylation reactions as good substrates when better consensus sequences [i.e., (S/T)-P-X-(R/K)] are absent.

The above results suggested the possibility that both S^{696}-PEK and S^{787}PSK sequences could be phosphorylated by cdc2 kinase. To confirm this, we produced synthetic peptides containing these sequences; RR-KELPPSPEKK (corresponding to MAP4 amino acid sequence 691−700) and RR-PEKRASPSKP (MAP4 amino acid sequence 782−791). Two arginine residues were added to the N-terminus of each peptide, to increase the positive charge in kinase assays using phosphocellulose filter paper. Both peptides were indeed good substrates for cdc2 kinase *in vitro* (data not shown). When the catalytic subunit of cyclic AMP-dependent protein kinase was used as a source of the kinase, minimum phosphate incorporation was detected.

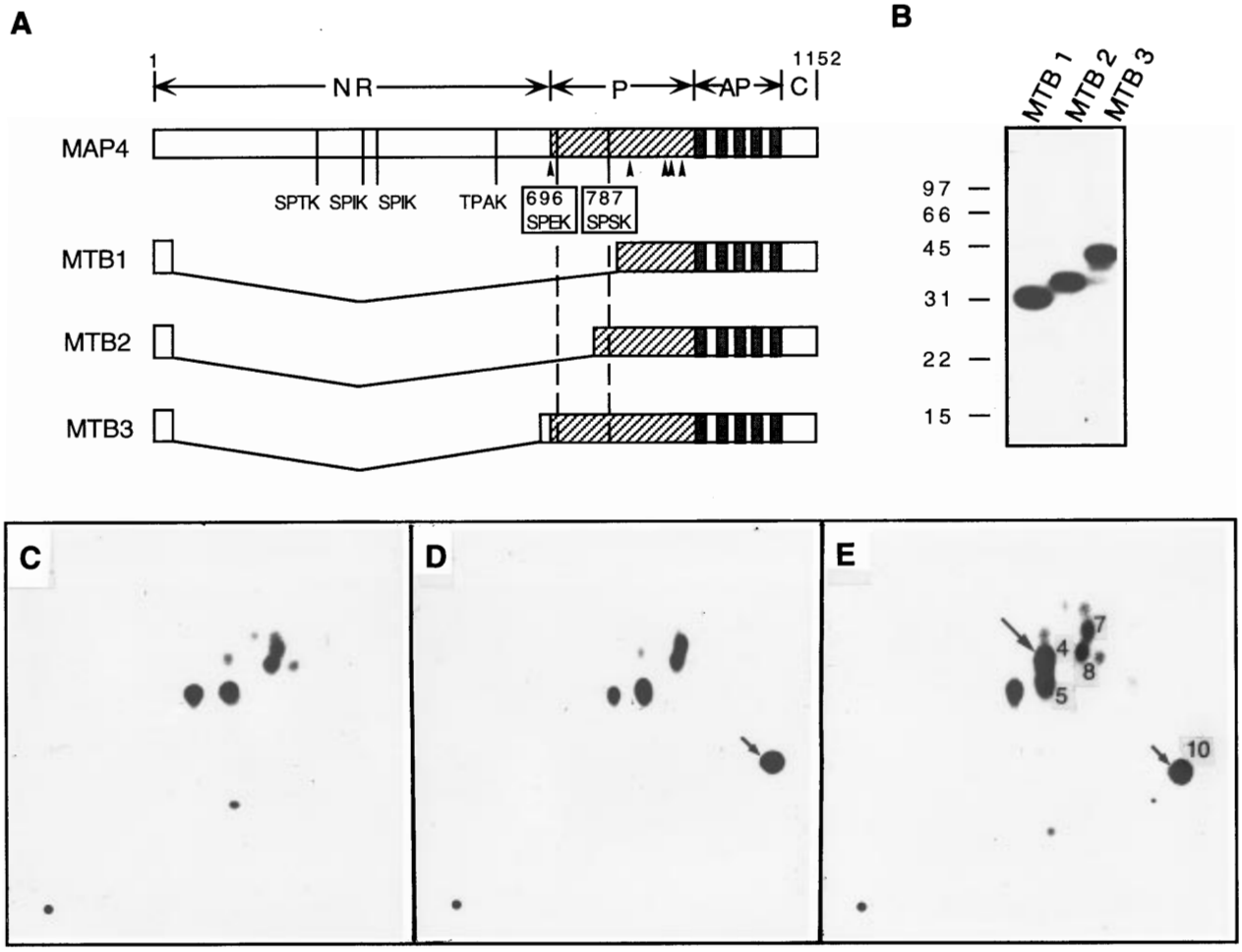

FIGURE 3: Identification of two cdc2 kinase phosphorylation sites in the proline-rich region of human MAP4. (A) Molecular structure of human MAP4 and location of cdc2 kinase consensus phosphorylation sites. Three MAP4 C-terminal fragments used to identify the phosphorylation sites are also shown. Human MAP4, composed of 1152 amino acids, can be divided into at least four regions; the amino-terminal half composed of the projection region (NR), the proline-rich basic region (P, striped), the assembly-promoting (AP) region composed of microtubule-binding repeats (hatched), and the extreme carboxy-terminal segment (C). Six (S/T)-P-X-(K/R) consensus motifs for phosphorylation by cdc2 kinase are present in the human MAP4 molecule; four are in the NR and two are in the P region. We focused on the two consensus phosphorylation sites within the P-region, enclosed by a square in the figure. Three C-terminal MAP4 fragments were constructed so that each contains neither, one, or both of the consensus sequences within the P-region. These fragments are called MTB1 (amino acid residues 800−1152, containing neither consensus sequence), MTB2 (amino acid sequence 763−1152, containing the S^{787}PSK sequence), and MTB3 (amino acid sequence 668−1152, containing both S^{696}PEK and S^{787}PSK sequences). (B) Phosphorylation of three MAP4 fragments by cdc2 kinase. The MAP4 fragments (40 μg/mL) phosphorylated in the presence of [γ-^{32}P]ATP by cdc2 kinase (0.5 μg/mL) were autoradiographed after SDS−PAGE. All three fragments were phosphorylated by cdc2 kinase regardless of the number of consensus sequences they contain. (C−E) 2D phosphopeptide map of the three MAP4 fragments, after *in vitro* phosphorylation by cdc2 kinase. Phosphorylated MTB1, MTB2, and MTB3 fragments were excised from the gel, and after digestion with lysylendopeptidase they were subjected to 2D phosphopeptide mapping (C−E). (C) MTB1; (D) MTB2; (E) MTB3. The spot present within MTB3 (large arrow in E), but absent from both MTB2 and MTB1 probably corresponds to the phosphopeptide containing the S^{696}PEK. The spot missing only in MTB1 may correspond to the phosphopeptide containing S^{787}PSK (arrow in D and E). To help to correlate each spot in this figure with those of Figure 2, spots in MTB3 (E) are labeled according to the number in Figure 2D.

Phosphorylated synthetic peptides were digested with lysylendopeptidase, and their migration was compared in 2D phosphopeptide maps to MAP4 or MTB3 phosphorylated *in vitro* by cdc2 kinase. Because the two synthetic peptides contain lysine residues at both ends of their phosphorylation sites, the digestion should produce the same phosphopeptides as phosphorylated MAP4 and MTB3. Migration of phosphorylated S^{696}PEK and S^{787}PSK peptides is shown in Figure 4A and B. The mixture of each with digested phosphopeptides from MAP4 or from MTB3 is shown in Figure 4C−F, respectively. Phosphorylated S^{696}PEK and S^{787}PSK peptides comigrated precisely with spots 4 and 10, respectively, demonstrating that these two sites are in fact the major phosphorylation sites in mitotic MAP4.

M-Phase-Specific and Cell Cycle-Independent Phosphorylation of MAP4

To investigate the phosphorylation state of these two sites *in vivo*, we produced polyclonal antibodies against a phosphorylated peptide, KELPPS(PO$_4$)PEKK or PEKRAS(PO$_4$)PSKP, conjugated with keyhole limpet hemocyanin. Both antibodies reacted with MAP4 prepared from mitotic HeLa cells (Figure 5A, lanes 4 and 7). This reaction was abolished by dephosphorylation of mitotic MAP4 with alkaline phosphatase (Figure 5A, lanes 5, 6, 8, and 9), indicating that these are phosphorylation-dependent epitopes. The specificity of antibodies was further examined by adsorption with the antigen peptide; reaction of anti-phospho-S^{696}PEK antibody with mitotic MAP4 was blocked by

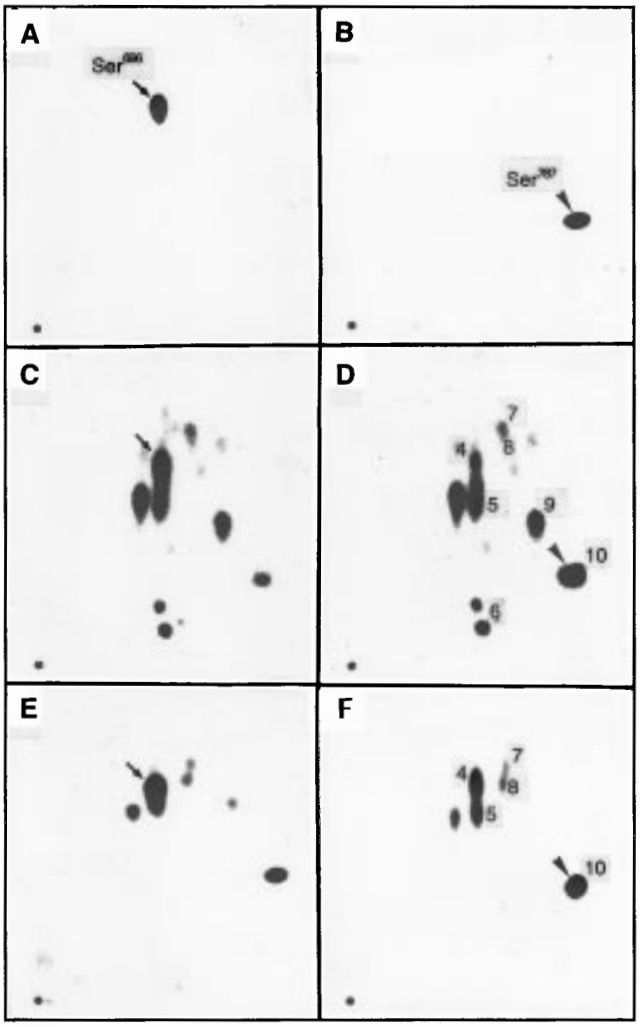

FIGURE 4: Identification of the phosphopeptide spots containing S[696]PEK and S[787]PSK sequences in 2D phosphopeptide mapping. The synthetic peptides, HeLa MAP4 and MTB3 were phosphorylated by cdc2 kinase *in vitro*. Phosphorylated peptides were bound to phosphocellulose filter paper; the paper was washed in 1% phosphoric acid five times, and then spots were released by digestion with lysylendopeptidase in 50 mM ammonium bicarbonate. Phosphopeptides of HeLa MAP4 and MTB3 were prepared as described in Figures 2 and 3. 2D phosphopeptide mapping was performed as described in Figure 3. 2D phosphopeptide map of the phosphorylated S[696]PEK peptide (A, arrow), the phosphorylated S[787]PSK peptide (B, arrowhead), the mixture of phosphorylated MAP4 peptides and S[696]PEK peptide (C), the mixture of phosphorylated MAP4 peptides and S[787]PSK peptide (D), the mixture of phosphorylated MTB3 peptides and S[696]PEK peptide (E), and the mixture of phosphorylated MTB3 peptides and S[787]PSK peptide (F). Arrows in A, C, and E indicate the spot of the phosphorylated S[696]PEK peptide; arrowheads in B, D, and E indicate the spot of the phosphorylated S[787]PSK peptide. The other spots in D and F are labeled according to Figure 2.

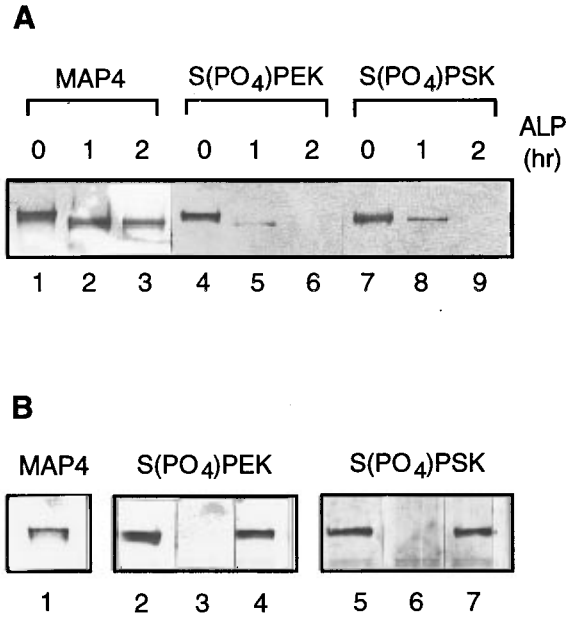

FIGURE 5: Specificity of anti-phospho-S[696]PEK and anti-phospho-S[787]PSK antibodies. (A) Immunoblotting of mitotic HeLa MAP4 with anti-bovine MAP4, anti-phospho-S[696]PEK and anti-phospho-S[787]PSK antibodies (lanes 1, 4, and 7). Both antibodies against the phosphorylated epitope reacted with MAP4 in mitotic HeLa cells. Dephosphorylation of MAP4 by *E. coli* alkaline phosphatase abolished the reaction with the anti-phospho-S[696]PEK and the anti-phospho-S[787]PSK antibodies (lanes 5, 6, 8, and 9). (B) Adsorption of antibodies with an antigen peptide. The anti-phospho-S[696]PEK and the anti-phospho-S[787]PSK antibodies were incubated with the phosphorylated antigen peptide or the unphosphorylated version of the antigen peptide and then reacted with the mitotic HeLa MAP4. The reaction of both antibodies with mitotic MAP4 was blocked by preincubation with the phosphopeptide used as an antigen (lane 3 and 6) but not with the unphosphorylated peptide (lane 4 and 7). Lanes 2 and 5 are blotted with untreated antibodies. Blotting with phosphorylation-independent MAP4 antibodies is shown in lane 1.

preincubation with the phospho-S[696]PEK peptide but not with the unphosphorylated S[696]PEK peptide (Figure 5B, lanes 3 and 4). Similarly, the reaction of anti-phospho-S[787]PSK antibody with mitotic MAP4 disappeared when antibodies were preincubated with the phospho-S[787]PSK peptide, but not when the unphosphorylated S[787]PSK peptide was used in the preincubation (Figure 5B, lanes 6 and 7). These results indicate that these antibodies specifically recognize the phosphorylated form of MAP4 at Ser-696 in the SPEK sequence and Ser-787 site in the SPSK sequence, respectively.

We used these antibodies to examine phosphorylation states of Ser-696 and Ser-787 in HeLa MAP4 during cell cycle progression. HeLa cells at S to M-phase were prepared by a procedure involving the thymidine block at S-phase, release from the block, and the nocodazole block of M-phase. Extracts of cells synchronized in this way showed that histone H1 kinase activity reached a maximum 12−13 h after thymidine release (Figure 6A), when >90% of the cells were in M-phase (data not shown). The mobility of MAP4 on SDS−PAGE was decreased gradually, in parallel with the increase in H1 kinase activity as determined by immunoblots labeled with phosphorylation-independent anti-MAP4 antibody (Figure 6B). In contrast to the anti-phospho-S[787]PSK antibody, which recognized mitotic MAP4 specifically (Figure 6B), the anti-phospho-S[696]PEK antibody reacted with MAP4 prepared from any phases of the cell cycle from S to M (Figure 6B).

Interphase phosphorylation at Ser-696 was confirmed by *in vivo* metabolic labeling of MAP4 (Figure 7). Asynchronous, log phase HeLa cells were cultured in [^{32}P]orthophosphate for 3 h as described above. MAP4 was prepared from heat-stable supernatants of cell extracts by binding to microtubules, just as we did to prepare mitotic MAP4. Two major phosphopeptides were identified in 2D phosphopeptide mapping of log phase MAP4 together with faint mitotic phosphorylation spots (Figure 7A). The upper spot comigrated with the phosphorylated S[696]PEK peptide (Figure 7B), whose sequence contains no other Ser, Thr, or Tyr residue

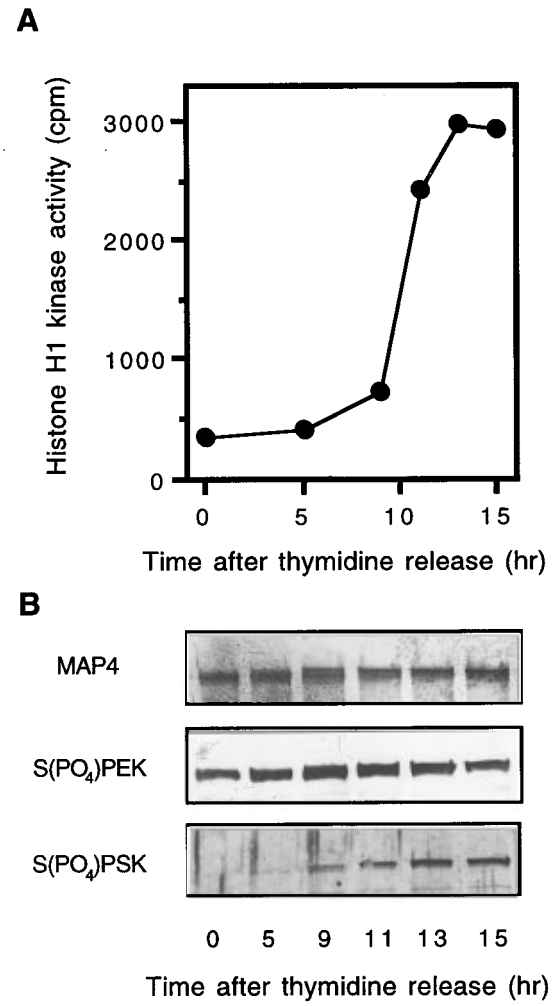

FIGURE 6: M-phase-dependent and cell cycle-independent phosphorylation of MAP4. HeLa cells synchronized at S phase by the thymidine block were allowed to progress to M-phase by release from thymidine block and arrest in nocodazole treatment. (A) Time course of histone H1 kinase activity after thymidine release. (B) Blotting of HeLa cell extracts from S- to M-phase with anti-bovine MAP4, anti-phospho-S^{696}PEK, and anti-phospho-S^{787}PSK antibodies. While the anti-phospho-S^{787}PSK antibody recognized only mitotic MAP4, the anti-phospho-S^{696}PEK antibody reacted with MAP4 in HeLa cells throughout S- to M-phase.

except Ser696. These results suggest that Ser-696 of MAP4 is phosphorylated in interphase HeLa cells. The identity of the lower spots is unknown at this time; it might correspond to spot 5 in Figure 3A which was also detected in 2D phosphopeptide mapping of MTB1 phosphorylated by cdc2 kinase *in vitro*. Alternatively, we cannot exclude the possibility that this interphase phosphopeptide constitutes an entirely different peptide that adventitiously comigrates with the M-phase peptide at spot 5.

To test the possibility that MAP4 is also phosphorylated by cyclin-dependent kinase(s) during interphase, the effect of BL-I on interphase phosphorylation was examined: 50 μM BL-I was added to the medium of asynchronous cell culture at the time when [^{32}P]orthophosphate was added, and the 2D phosphopeptide map of isolated MAP4 was obtained (Figure 7C). Phosphorylation at Ser-696 and spot 5 was suppressed by BL-I, indicating that cdks may be involved in interphase phosphorylation of MAP4, as well as in mitosis. At this time, the identity of these cdks is unknown, although it is likely to be cdk2 because other cdks are not inhibited by BL-I (*49*).

DISCUSSION

Cdc2 Kinase Is the Major Kinase That Phosphorylates MAP4 in HeLa Cells at Mitosis

In this paper, we have used several lines of evidence to demonstrate that MAP4 is phosphorylated primarily by cdc2 kinase in mitotic HeLa cells. First, phosphorylation of MAP4 increased at mitosis, the stage at which cdc2 kinase is normally activated. Second, we have utilized a specific inhibitor of cdc2 kinase and cdk2 kinase, BL-I, to inhibit phosphorylation of MAP4 both in mitotic HeLa cells (*in vivo*) and in miotic HeLa cell extracts (*in vitro*). Third, we showed that five out of eight *in vivo* phosphorylation spots were identical to those phosphorylated by cdc2 kinase *in vitro*. The present results clearly confer physiological significance on our previous *in vitro* finding, that $p34^{cdc2}$/cyclin B kinase increased microtubule dynamics through phosphorylation of MAP4 (*14*).

Thus far, MAP4 is one of a few proteins likely to be *in vivo* substrates for cdc2 kinase. There are many proteins that have been shown to be phosphorylated by cdc2 kinase, including histone H1, nuclear lamin, caldesmon, vimentin, nucleolin, EF1-γ, CENP-E, etc. (*52*, *56*). However, except for a few proteins including nuclear lamin and caldesmon (*57*, *58*) many of these have not been clearly shown to be *in vivo* substrates for cdc2 kinase. This is partly due to the overlap in substrate specificity among cdc2 kinase, MAP kinase, and glycogen synthase kinase 3 (GSK3). These three kinases are known to be proline-directed kinases, which prefer the motif of Ser or Thr followed by Pro as a substrate (*50*, *51*). This is particularly troublesome with embryonic cells in which both of cdc2 kinase and MAP kinase are activated at mitosis (*9*, *33*). Even if a particular protein is phosphorylated at mitosis *in vivo* on the same sites as those phosphorylated by cdc2 kinase *in vitro*, it is not possible to conclude that the protein is an *in vivo* substrate for cdc2 kinase because of the overlapping substrate specificity with MAP kinase. For MAP4, another question to be addressed is the relevance of *in vitro* phosphorylation experiments previously performed with MAP kinase and protein kinase C to MAP4's *in vivo* mitotic phosphorylation (*12*, *32*). Phosphorylation by these kinases reduces the microtubule-polymerizing activity of MAP4, just as phosphorylation by cdc2 kinase does (*14*).

We avoided potential problems of attributing phosphorylation to one or more kinases other than cdc2 kinase, by using somatic cultured cells as experimental material, and by using a cdc2 kinase selective inhibitor, BL-I. The activation of MAP kinase and protein kinase C at mitosis in mammalian cultured cells is still a controversial question. Although there are a few reports describing the activation of a type of MAP kinase at late G2, at a stage earlier than cdc2 kinase (*59*, *60*), the major activation of MAP kinase in somatic cells occurs at the time of growth stimulation in G1 (*61*). Similarly, although a few recent reports suggest a possible mitotic function of protein kinase C (*62*, *63*), this kinase has not been considered to be under cell cycle control. Inhibition experiments with BL-I which inhibits cdk family kinases, but not other kinases; both *in vivo* and *in vitro* exclude the possibility of MAP kinase, protein kinase C, and GSK3 as the major mitotic MAP4 kinase in HeLa cells. Phosphorylation of MAP4 was inhibited at 20−50 μM BL-I which is

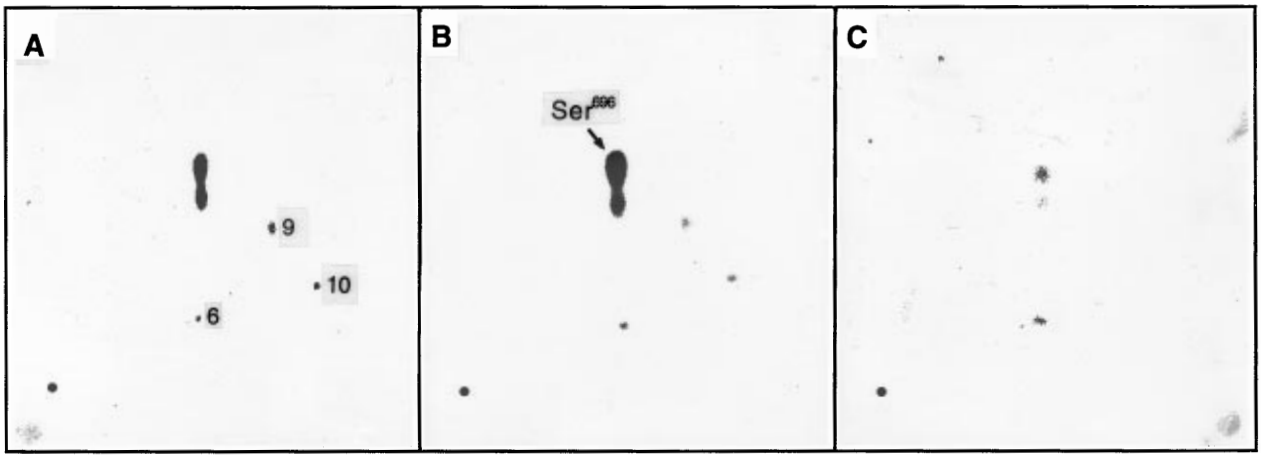

FIGURE 7: 2D phosphopeptide mapping of HeLa MAP4 metabolically labeled in interphase and the effect of BL-I on interphase phosphorylation. Asynchronous HeLa cells were cultured for 3 h in the presence of [^{32}P]orthophosphate. MAP4 was prepared from a heat-stable supernatant fraction of the HeLa extract by binding to microtubules and was then subjected to 2D phosphopeptide mapping (A) as described in Figure 3. Minor spots (labeled as 6, 9, and 10) comigrating with mitotic phosphorylation spots are most likely derived from a small population of mitotic cells present in asynchronous cultures. (B) Mixture of the interphase-phosphorylated MAP4 and the phosphorylated S^{696}PEK peptide (arrow). To examine involvement of cdks in interphase phosphorylation, BL-I was added to the culture medium during the period of metabolic labelling. (C) 2D map of MAP4 labeled in the presence of 50 μM BL-I. Faint spot observed at the upper-middle portion in C is the peptide containing Ser^{696}.

Table 1: MAP4 Phosphorylation Spots: Their Intensities and Their Phosphorylation Site or Domain

	phosphorylation			
spot number	at M-phase	in interphase	by cdc2 kinase *in vitro*	site or domain in MAP4
1	0.74[a]			?
2	0.22			?
3	0.27			?
4	1	1	0.77	Ser-696
5	0.34	0.66	1	AP[b] or Pro[c]
6	0.62	0.04	0.24	NR[d]
7			0.55	AP or Pro
8			0.36	AP or Pro
9	0.75	0.14	0.90	NR
10	0.54	0.08	0.87	Ser787

[a] Spot intensities estimated from 2D phosphopeptide map images by a BAS2000 image analyzer. Most intense spot in each 2D map was assigned to be 1. [b] Assembly-promoting, repeat-region of MAP4. [c] Proline-rich region of MAP4. [d] N-terminal half of MAP4.

insufficient for inhibition of MAP kinase and GSK3β (*49*, *64*). Furthermore, the 2D phosphopeptide maps of MAP4 phosphorylated by MAP kinase and GSK3β both differed significantly from that of mitotic phosphorylation of MAP4. Taken together, these results make it unlikely that either of these kinases is the major mitotic MAP4 kinase, although we cannot exclude the possibility that some of these other kinases phosphorylate unidentified sites (see below) and also participate in modulation of the microtubule-stabilizing activity of MAP4 synergistically with cdc2 kinase.

Phosphorylation Sites in MAP4 at Mitosis

We identified at least eight *in vivo* phosphorylation spots in mitotic MAP4. Here, we can speculate on possible phosphorylation sites and the kinase responsible on the basis of the results obtained with the *in vitro* phosphorylation of MAP4 and fragments MTB1−3 by cdc2 kinase (Table 1). (i) Five phosphorylation spots (4−6, 9, and 10) were generated by phosphorylation with cdc2 kinase (Figure 2B). BL-I inhibited phosphorylation at these sites in the mitotic HeLa cell extract (data not shown), making the *in vivo* cdc2 kinase-dependent phosphorylation at these sites likely. (ii) Three (4, 5, and 10) of the five sites were located in the C-terminal half of the MAP4 molecule (Figure 3E). Spot 9, which appeared in 2D phosphopeptide mapping of MAP4, but not in MTB3, phosphorylated by cdc2 kinase, must be present in the N-terminal (NR) domain (Figure 2B and 3E). Spot 6 separated into two spots depending on some experiments (Figure 4C and D). Considering that these spots were not detected in MTB3 phosphorylated by cdc2, spot 6 may also be a fragment derived from the N-terminal half. Comparing to other spots (4, 5, 9, and 10) which were phosphorylated a similar extent both *in vivo* and *in vitro*, spot 6 was phosphorylated *in vivo* more intensely than *in vitro* by cdc2 kinase. Spot 6 could be phosphorylated by kinases other than cdc2 kinase at mitosis. (iii) Spots 4 and 10 were shown to contain Ser-696 and Ser-787, respectively (Figure 4). (iv) Spot 5 might constitute phosphorylation at either SP (Ser-825) or three TP (Thr-892, Thr-901, and Thr-917) sequences located between Ser-787 and the microtubule-binding repeat sequences (Figure 3A). The (S/T)-P motif can also be phosphorylated by cdc2 kinase depending on the protein context (*51*). Aizawa et al. (*10*) reported cdc2 kinase-dependent phosphorylation of an SP or TP site in bovine MAP4, though these sites are not conserved between bovine and human MAP4 (*26*, *27*, *53*). Mitotic phosphorylation of the (S/T)-P motif is also shown when tau, a brain MAP with a molecular structure similar to MAP4, was transfected into Chinese hamster ovary cells (*65*). (v) Spots 1−3 were not produced by phosphorylation with cdc2 kinase, suggesting that these spots are targeted by kinases other than cdc2 kinase. Identification of these phosphorylation sites and the protein kinase phosphorylating them is currently underway.

Interphase Phosphorylation at Ser-696 of MAP4

Ser-696 and spot 5 in MAP4, both of which were phosphorylated *in vitro* and at mitosis by cdc2 kinase, were also phosphorylated in interphase HeLa cells. This is the first evidence for the interphase phosphorylation of MAP4. When BL-I was applied to interphase cells, phosphorylation

at Ser-696 was suppressed by BL-I. BL-I can inhibit cdk2, cdk5, and cdc2 kinase but not cdk4 or cdk6 (*49*, *66*). Because cdk5 activity has not been detected in proliferating cells (*67*), cdk2 could be the BL-I sensitive kinase acting on MAP4 in interphase. cdk2 is activated by binding to cyclin E at G1/S transition and by binding to cyclin A during S-phase (*56*). We detected interphase phosphorylation of Ser-696 with asyncronously cultured cells by metabolic labeling and S- to M-phase phosphorylation with synchronized cells by immunoblotting. To determine the interphase MAP4 kinase exactly, it may be necessary to examine the phosphorylation state of Ser-696 and spot 5 in MAP4 during G1 to S phase.

Ser-787 Could Be One of the Critical Phosphorylation Sites for Regulation in Microtubule Dynamics at Mitosis

Phosphorylation by cdc2 kinase decreased the microtubule-stabilizing ability of MAP4, suggesting that there are critical phosphorylation sites among the five major cdc2 kinase-dependent phosphorylation sites [spots 4 (Ser-696), 5, 6, 9, and 10 (Ser-787)]. Phosphorylation in the C-terminal half [spots 4 (Ser-696), 5, and 10 (Ser-787)] would appear to be more important for MAP4 binding to microtubules than those (spots 6 and 9) in the N-terminal projection domain. All three C-terminal phosphorylation sites would be located in the proline-rich region, if spot 5 corresponds to one of SP or TP motif in the N-terminal region next to the microtubule-binding repeats. The importance of the proline-rich region in microtubule-binding was originally demonstrated in *in vitro* polymerization experiments by Aizawa et al. (*53*), and this was recently confirmed *in vivo* by Olsen et al. (*54*) using GFP-MAP4 chimera proteins.

Phosphorylation at three sites in the proline-rich region (Ser-696, Ser-787, and spot 5) may not necessarily contribute equally to the destabilization of microtubules associated with MAP4. MAP4 prepared from interphase HeLa cells had a strong microtubule-stabilizing ability (*14*), nevertheless interphase MAP4, at least in part, was phosphorylated at Ser-696 and at the unidentified site migrating as spot 5. Further phosphorylation on Ser-787 by cdc2 kinase might greatly reduce the microtubule-stabilizing ability of MAP4. This suggests the possibility that Ser-787 plays important roles more than on its own or in combination with Ser-696 and the site in spot 5, in stabilizing microtubules. The fact that the S^{787}PSK sequence is conserved in all mammalian MAP4 molecules sequenced to date supports this notion (*26*, *27*). Further, in our preliminary binding experiments using MAP4 C-terminal fragments, MTB1 showed weaker binding to microtubule than MTB2 and MTB3 (data not shown), suggesting that the N-terminal part of the Proline-rich region is necessary for binding to microtubules. Its phosphorylation could provide a mechanism to regulate MAP4's affinity for microtubules. To reveal an exact role for phosphorylation at Ser-696 and Ser-787, it will be necessary to generate mutant MAP4 proteins whose Ser residues are changed to Glu or Ala to mimic phosphorylated or unphosphorylated forms.

MAP4 Function in in Vivo Microtubule Dynamics

Recent immunodepletion experiments by Wang et al. (*68*) raised the question of the role of MAP4 in microtubule stabilization *in vivo*. Wang et al. (*68*) depleted MAP4 by injecting MAP4 antibody into living cells. In these experiments, Wang et al. found that MAP4 depletion did not affect any activities examined, including microtubule turnover and ability to enter into M-phase. These results suggest the possibility that MAP4 actually does not contribute significantly to microtubule stabilization *in vivo*. On the other hand, it has been shown by overexpression or microinjection experiments of MAP4 into cultured cells that MAP4 actually has a microtubule-stabilizing ability *in vivo* (*36*, *69*). The amount of MAP4 in cultured cells is much lower than the amount of its counterparts in neurons—MAP2 or tau. It is possible that the microtubule stabilization contributed by MAP4 would be undetectable under the experimental system by Wang et al. (*68*). Alternatively, there could be functionaly redundant MAPs that are also in those cells studied by Wang et al. Novel MAPs have recently been reported in cultured cells (*46*−*48*).

Immunodepletion of MAP4 did not inhibit entry of cells into mitosis (*68*), though timing of this event was not examined. Depletion of MAP4 may have a similar effect to M-phase phosphorylation with respect to decreasing the microtubule-stabilization ability. Therefore, it may not be so curious that MAP4-depleted cells can pass through mitosis normally. To investigate roles of mitotic phosphorylation of MAP4, introduction of nonphosphorylatable mutants of MAP4 into cells would be useful.

Several laboratories suggested recently that oncoprotein 18 (Op18) (also named p19, stathmin, or leukemia-associated protein 18) affects microtubule dynamics *in vivo* and that this activity is modulated by phosphorylation with cdc2 kinase (*70*−*72*). Belmont and Mitchison showed that Op18 increases the rate of catastrophe, that is, the transition from growing phase to shortening phase, by binding to tubulin (*70*). They postulated initially that mitotic microtubule-destabilization with the activity of Op18 activated by phosphorylation at mitosis. However, more recent papers showed that phosphorylation at cdc2 target sites abolished the activity of Op18, while an unphosphorylated form of Op18 in interphase had strong activity (*71*, *72*). This result is inconsistent with the microtubule dynamics observed during the cell cycle. In any case, it is likely that both microtubule-destabilizing proteins and microtubule-stabilizing proteins such as MAP4, exist within cells. Although it is not known yet how they coordinate, microtubule dynamics must be regulated via mechanism that involves both microtubule-destabilizing and -stabilizing proteins.

ACKNOWLEDGMENT

We express our thanks to Dr. N. Lomax (Drug Synthesis and Chemistry Branch, National Cancer Institute, MD) for providing paclitaxel, to Dr. Eisuke Nishida (Kyoto University, Kyoto) for providing *Xenopus* MAP kinase cDNA, to K. Wada for his help in a BAS image analyzer operation, and to K. Nonoyama for his help in a purification of MAP4 fragments and MAP kinase.

REFERENCES

1. Mitchison, T. (1988) *Annu. Rev. Cell. Biol. 4*, 527−549.
2. McIntosh, J. R., and Koonce, M. P. (1989) *Science 246*, 622−628.
3. Centonze, V., and Borisy, G. G. (1990) *J. Cell Sci. 95*, 405−411.

4. Verde, F., Labbe, J.-C., Doree, M., and Karsenti, E. (1990) *Nature 343*, 233−238.
5. Buendia, B., Draetta, G., and Karsenti E. (1992) *J. Cell Biol. 116*, 1431−1442.
6. Gliksman, N. R., Parsons, S. F., and Salmon, E. D. (1992) *J. Cell Sci. 119*, 1271−1276.
7. Belmont, L. D., Hyman, A. A., Sawin, K. E., and Mitchison, T. J. (1990) *Cell 62*, 579−589.
8. Verde, F., Dogterom, M., Stelzer, E., Karsenti, E., and Leibler S. (1992) *J. Cell Biol. 118*, 1097−1108.
9. Gotoh, Y., Nishida, E., Matsuda, S., Shiina, N., Kosaka, H., Shiokawa, K., Akiyama, T., Ohta, K., and Sakai, H. (1991) *Nature 349*, 251−254.
10. Aizawa, H., Kamijo, M., Ohta, Y., Mori, A., Okuhara, K., Kawasaki, H., Murofushi, H., Suzuki, K., and Yasuda, Y. (1991) *Biochem. Biophys. Res. Commun. 179*, 1620−1626.
11. Faruki, S., Doree, M., and Karsent, E. (1992) *J. Cell Sci. 101*, 69−78.
12. Hoshi, M., Ohta, K., Gotoh, Y., Mori, A., Murofushi, H., Sakai, H., and Nishida, E. (1992) *Eur. J. Biochem. 203*, 43−52.
13. Shiina, N., Moriguchi, T., Ohta, K., Gotoh, Y., and Nishida, E. (1992) *EMBO J. 11*, 3977−3984.
14. Ookata, K., Hisanaga, S., Bulinski, J. C., Murofushi, H., Aizawa, H., Itoh, T. J., Hotani, H., Okumura, E., Tachibana, K., and Kishimoto, T. (1995) *J. Cell Biol. 128*, 849−862.
15. Olmsted, J. B. (1986) *Annu. Rev. Cell Biol. 2*, 421−457.
16. Vallee, R. B. (1990) *Cell Motil. Cytoskel. 15*, 204−209.
17. Chapin, S. J., and Bulinski, J. C. (1992) *Cell Motil. Cytoskel. 23*, 236−243.
18. Pryer, N. K., Walker, R. A., Skeen, V. P., Bourns, B. D., Soboerio, M. F., and Salmon, E. D. (1992) *J. Cell Sci. 103*, 965−976.
19. Kanai, Y., Chen, J., and Hirokawa, N. (1992) *EMBO J. 11*, 3953−3961.
20. Itoh, T. J., and Hotani, H. (1994) *Cell Struct. Funct. 19*, 279−290.
21. Drechel, D. N., Hyman, A. A., Cobb, M. H., and Kirschner, M. (1992) *Mol. Biol. Cell 3*, 1141−1154.
22. Biernat, J., Gustke, N., Drewes, G., Mandelkow, E.-M., and Mandelkow, E. (1993) *Neuron 11*, 153−163.
23. Bramblett, G. T., Goedert, M., Jakes, R., Merrick, S. E., Trojanowski, J. Q., and Lee, V. M.-Y. (1993) *Neuron 10*, 1089−1099.
24. Bulinski, J. C., and Borisy, G. G. (1980) *J. Biol. Chem. 255*, 11570−11576.
25. Weatherbee, J. A., Sherline, P., Mascardo, R. N., Izant, J. G., Luftig, R. B., and Weihing, R. R. (1982) *J. Cell Biol. 92*, 155−163.
26. West, R. R., Tenbarge, K. M., and Olmsted, J. B. (1991) *J. Biol. Chem. 266*, 21886−21896.
27. Chapin, S. J., Yu, C.-M. L., and Bulinski, J. C. (1995) *Biochemistry 34*, 2289−2301.
28. Bulinski, J. C. (1994) in *Microtubules* (Hyams, J. S., and Lloyd, C. W., Eds.) pp 167−182, Wiley-Liss, New York.
29. Vandre, D. D., Centonze, V. E., Peloquin, J., Tombes, R. M., and Borisy, G. G. (1991) *J. Cell Sci. 98*, 577−588.
30. Tombes, R. M., Peloquin, J. G., and Borisy, G. G. (1991) *Cell Regul. 2*, 861−874.
31. Olmsted, J. B., Stemple, L., Saxton, W. M., Neighbors, B. W., and McIntosh, J. R. (1989) *J. Cell Biol. 109*, 211−223.
32. Mori, A., Aizawa, H., Saido, T. C., Kawasaki, H., Mizuno, K., Murofushi, H., Suzuki, K., and Sakai, H. (1991) *Biochemistry 30*, 9341−9346.
33. Shibuya, E. K., Boulton, T. G., Cobb, M. H., and Ruderman, J. V. (1992) *EMBO J. 11*, 3963−3975.
34. Murofushi, H., Kotani, S., Aizawa, H., Maekawa, S., and Sakai, H. (1987) *J. Biochem. 102*, 1101−1112.
35. Studier, F. W., Rosenberg, A. W., Dunn, J. J., and Dubendorff, J. W. (1990) *Methods Enzymol. 185*, 60−89.
36. Nguyen, H. L., Chari, S., Gruber, D., Lue, C.-M., Chapin, S. J., and Bulinski, J. C. (1997) *J. Cell Sci. 110*, 281−294.
37. Shelanski, M. L. F., Gaskin, F., and Cantor, C. R., (1973) *Proc. Natl. Acad. Sci. U.S.A. 70*, 765−768.
38. Weingarten, M. D., Lockwood, A. H., Hwo, S. Y., and Kirschner, M. W. (1975) *Proc. Natl. Acad. Sci. U.S.A. 72*, 1858−1862.
39. Vallee, R. B. (1982) *J. Cell Biol. 92*, 435−442.
40. Kusubata, M., Tokui, T., Matsuoka, Y., Okumura, E., Tachibana, K., Hisanaga, S., Kishimoto, T., Yasuda, H., Kamijo, M., Ohba, Y., Tsujimura, K., Yatani, R., and Inagaki, M. (1992) *J. Biol. Chem. 267*, 20937−20942.
41. Okumura, E., Sekiai, T., Hisanaga, S., Tachibana, K., and Kishimoto, T. (1996) *J. Cell Biol. 132*, 125−135.
42. Fukuda, M., Gotoh, Y., Tachibana, T., Dell, K., Hattori, S., Yoneda, Y., and Nishida, E. (1995) *Oncogene 11*, 239−244.
43. Boyle, W. J., Geer, P., and Hunter, T. (1991) *Methods Enzymol. 201*, 110−149.
44. Laemmli, U. K. (1970) *Nature 227*, 680−685.
45. Ookata, K., Hisanaga, S., Okano, T., Tachibana, K., and Kishimoto, T. (1992) *EMBO J. 11*, 1763−1772.
46. Bulinski, J. C., and Bossler, A. (1994) *J. Cell Sci. 107*, 2839−2849.
47. Masson, D., and Kreis, T. E. (1993) *J. Cell Biol. 123*, 357−371.
48. Masson, D., and Kreis, T. E. (1995) *J. Cell Biol. 13*, 1015−1024.
49. Kitagawa, M., Higashi, H., Takahashi, S. I., Okabe, T., Ogino, H., Taya, Y., Nishimura, S., and Okuyama, A. (1994) *Oncogene 9*, 2549−2557.
50. Woodgett, J. R. (1991) *Trends Biochem. Sci. 16*, 177−181.
51. Nigg, E. A. (1993) *Trends Cell Biol. 3*, 296−301.
52. Moreno, S., and Nurse, P. (1990) *Cell 61*, 549−551.
53. Aizawa, H., Emori, Y., Mori, A., Murofushi, H., Sakai, H., and Suzuki, H. (1991) *J. Biol. Chem. 266*, 9841−9846.
54. Olsen, K. R., McIntosh, J. R., and Olmsted, J. B. (1995) *J. Cell Biol. 130*, 639−650.
55. Aizawa, H., Emori, Y., Murofushi, H., Kawasaki, H., Sakai, H., and Suzuki, K. (1990) *J. Biol. Chem. 265*, 13849−13855.
56. Nigg, E. A. (1995) *BioEssays 17*, 471−480.
57. Matsumura, F., and Yamashiro, S. (1993) *Curr. Opin. Cell Biol. 5*, 70−76.
58. Moir, R. D., Spann, T. P., and Goldman, R. D. (1995) *Int. Rev. Cytol. 162B*, 141−182.
59. Tamemoto, H., Kadowaki, T., Tobe, K., Ueki, K., Izumi, T., Chatani, Y., Kohno, M., Kasuga, M., Yazaki, Y., and Akanuma, Y. (1992) *J. Biol. Chem. 267*, 20293−20297.
60. Heider, H., Hug, C., and Lucoco, J. M. (1994) *Eur. J. Biochem. 219*, 513−520.
61. Johnson, G. L., and Vaillancourt, R. R. (1994) *Curr. Opin. Cell Biol. 6*, 230−238.
62. Goss, V. L., Hocevar, B. A., Thompson, L. J., Stratton, C. A., Burns, D. J., and Fields, A. P. (1994) *J. Biol. Chem. 269*, 19074−19080.
63. Lehrich, R. W., and Forrest, J. N., Jr. (1994) *J. Biol. Chem. 269*, 32446−32450.
64. Hosoi, T., Uchiyama, M., Okumura, E., Saito, T., Ishiguro, K., Uchida, T., Okuyama, A., Kishimoto, T., and Hisanaga, S. (1995) *J. Biochem. 117*, 741−749.
65. Preuss, U., Doring, F., Illenberger, S., and Mandelkow, E.-M. (1995) *Mol. Biol. Cell 6*, 1397−1410.
66. Hisanaga, S., Uchiyama, M., Hosoi, T., Yamada, K., Honma, N., Ishiguro, K., Uchida, T., Dahl, D., Ohsumi, K., and Kishimoto, T. (1995) *Cell Motil. Cytoskel. 31*, 283−297.
67. Lew, J., and Wang, J. H. (1995) *Trends Biochem. Sci. 20*, 33−37.
68. Wang, X. M., Peloquin, J. G., Zhai, Y., Bulinski, J. C., and Borisy, G. G. (1996) *J. Cell Biol. 132*, 345−357.
69. Yoshida, T., Imanaka-Yoshida, K., Murofushi, H., Tanaka, J., Ito, H., and Inagaki, M. (1996) *Cell Motil. Cytoskel. 33*, 252−262.
70. Belmont, L. D., and Mitchison, T. J. (1996) *Cell 84*, 623−631.
71. Marklund, U., Larsson, N., Gradin, H. M., Brattsand, G., and Gullberg, M. (1996) *EMBO J. 15*, 5290−5298.
72. Horwitz, S. B., Shen, H.-J., He, L., Dittmar, P., Neef, R., Chen, J., and Schubart, U. K. (1997) *J. Biol. Chem. 272*, 8129−8132.

BI971251W